Leaf wax *n*-alkanes in modern plants and topsoils from eastern Georgia (Caucasus) – implications for reconstructing regional paleo-vegetation

Marcel Bliedtner[1], Imke K. Schäfer[1], Roland Zech[1,3], Hans von Suchodoletz[2]

[1]Institute of Geography and Oeschger Centre for Climate Change Research, University of Bern, Hallerstrasse 12, CH-3012 Bern, Switzerland
[2]Institute of Geography, University of Leipzig, Johannisallee 19a, D-04103 Leipzig, Germany
[3]Institute of Geography, University of Jena, Löbdergraben 32, D-07743 Jena, Germany

Correspondence to: Marcel Bliedtner (marcel.bliedtner@giub.unibe.ch)

Abstract.

Long-chain *n*-alkanes became increasingly used for paleoenvironmental studies during the last years as they have the great potential to reconstruct past changes in vegetation and climate. They mostly originate from leaf waxes of higher terrestrial plants, are relatively resistant against physical and chemical degradation and can thus serve as valuable biomarkers that are preserved in various sedimentary archives for at least millennial timescales. However, before any robust interpretation of the long-chain *n*-alkane patterns in sedimentary archives, reference samples from modern vegetation and topsoil material should be investigated at a regional scale. Apart from Central and South-Eastern Europe, such systematic regional studies on modern plant and topsoil material are still largely lacking.

To test the potential of leaf wax derived *n*-alkane patterns for paleoenvironmental studies in the semi-humid to semi-arid southern Caucasus region, we investigated the influence of different vegetation types on the leaf wax *n*-alkane signal in modern plants and topsoil material (0-5 cm) from eastern Georgia. We sampled (i) sites with grassland that included steppe, cultivated grassland and meadows, and (ii) sites that are dominated by deciduous hornbeam forests.

The *n*-alkane results show distinct and systematic differences between samples from sites with the different vegetation types: *n*-alkanes derived from sites with grassland are mainly dominated by C_{31}, while *n*-alkanes derived from sites with deciduous trees show high abundances of C_{29}. Thus, chain-length ratios allow to discriminate between these two different vegetation types and have a great potential when used for regional paleoenvironmental reconstructions. As degradation of organic matter can affect the leaf wax *n*-alkane distribution, we further present an updated end-member model that includes our results, accounts for degradation effects and enables semi-quantitative reconstructions of past vegetation changes in the southern Caucasus region.

1 Introduction

Long-chain *n*-alkanes (C_{25}-C_{35}) are produced as part of the epicuticular leaf waxes by terrestrial plants and serve as valuable biomarkers (Eglinton et al., 1962; Eglinton and Hamilton, 1967; Kolattukudy and Walton, 1973). Typically, leaf wax *n*-alkanes show a distinct odd-over-even predominance (OEP) (Eglinton and Hamilton, 1967), and their relative odd homo-

5 logue distribution might be used to differentiate between vegetation forms. The chain-lengths C_{27} and C_{29} are mainly produced by deciduous trees and shrubs, while C_{31} and C_{33} mainly derive from grasses and herbs (Marseille et al., 1999; Zech et al., 2009; Schwark et al., 2002). Because of their low water-solubility, chemical inertness and relative persistence against physical and chemical degradation, they stay well preserved in soils and sedimentary archives, at least over millennial time-scales (Eglinton and Eglinton, 2008). Up to now, long-chain *n*-alkanes have increasingly been applied to various paleoenvi-

10 ronmental archives such as lacustrine and marine sediments and loess-paleosol sequences (Schwark et al., 2002; Schefuß et al., 2003; Zhang et al., 2006; Liu and Huang, 2005; Schatz et al., 2011; Zech et al., 2009; Schäfer et al., 2016a) in order to reconstruct paleovegetation and -climate.

However, robust interpretations of long-chain *n*-alkanes in sedimentary archives need to be evaluated by modern, regional calibration studies on plant and topsoil material, but such calibration studies are still largely lacking. The need for regional

15 calibration studies is underlined by the fact that Bush and McInerney (2013) report no discrimination of modern vegetation patterns from different sites around the world using *n*-alkanes, and questioned whether *n*-alkane patterns are suitable to distinguish between different vegetation types at least on a global scale. In contrast, on a regional level some studies from Central and South-Eastern Europe prove the discrimination power for vegetation reconstruction by *n*-alkanes, although the most abundant *n*-alkane homologues show regional differences (Zech et al., 2009; Zech et al., 2013; Schäfer et al., 2016b). While

20 Schäfer et al. (2016a) report that C_{27} is the most abundant homologue produced under deciduous sites in humid Cental Europe, Zech et al. (2013) show that C_{29} is the dominant homologue under deciduous sites in more arid South-Eastern Europe. Moreover, several potential pitfalls can complicate the interpretation of long-chain *n*-alkanes, as there are wide species-specific variations (Diefendorf et al., 2011; Bush and McInerney, 2013), environmental factors (Hoffmann et al., 2013; Tipple and Pagani, 2013) and degradation effects (Buggle et al., 2010) that all can additionally influence the *n*-alkane pattern.

25 Thus, prior to the application of long-chain *n*-alkanes for paleovegetation reconstructions in sedimentary archives regional calibration sets from modern long-chain *n*-alkane patterns are necessary to i.) prove their leaf wax origin, and ii.) justify their discrimination power between grasses and deciduous trees.

This study evaluates long-chain *n*-alkane patterns of modern plant and topsoil material from eastern Georgia in the central-southern Caucasus region to test their leaf wax origin and chemotaxonomic potential, i.e. whether *n*-alkane abundances and

30 chain-length distributions can be used to discriminate between deciduous trees and grasses on a regional level. The leaf wax *n*-alkane pattern can be affected by degradation effects, but these effects can be checked and corrected for with regionally derived end-members (Zech et al., 2013; Schäfer et al., 2016b). Thus, we further aim to establish a regional calibration set and end-member model of *n*-alkanes for the southern Caucasus region as a base for future robust interpretations of leaf wax

n-alkane patterns derived from regional sediment archives. Such lacustrine, loess-paleosol, open-air archaeological or fluvial archives were increasingly investigated during the last years and could potentially be used for *n*-alkane derived vegetation reconstructions (Messager et al., 2013; Joannin et al., 2014; Suchodoletz et al., 2015; Wolf et al., 2016; Egeland et al., 2016).

2 Material and Methods

2.1 Geographical setting and field sampling

The semi-humid to semi-arid central southern Caucasus region is characterized by a small-scale pattern of different ecologic regions. Due to a rain-shadow that is caused by the high elevation of the Western and Central ranges of the Greater Caucasus and by the N-S-directed Likhi Range linking the Greater and Lesser Caucasus, there exists a significant climatic gradient with decreasing precipitation and more continental conditions going eastwards (Connor and Kvavadze, 2008). Our study of modern plant and topsoil material took place in eastern Georgia (see Fig. 1) at the end of the vegetation period in September 2016. We sampled 22 sites that are located along a N-S-directed transect with a length of ca. 65 km. The transect extends from the surroundings of Tbilisi in the south over the mid-mountain Kura-fold-and-thrust-belt (Forte et al., 2010) into the upper part of the Alazani valley in the north. The sampled grassland sites included steppe, cultivated grassland and meadows, and the deciduous sites were mainly dominated by hornbeam forests (see Fig. 2A for sample locations and supporting online material SOM-1 and 2 for site descriptions). At each site, we sampled plant material and the upper 0-5 cm of the topsoil.

The altitudes along the transect range between 445 and 1659 m a.s.l., mean annual temperatures between ca. 11.3 and 13.3°C and recent annual precipitation between ca. 600 and 1000 mm/a (unpublished precipitation map of W. Bagrationi Geographical Institute Tbilisi). Precipitation mainly falls in spring and early summer during convective events (Lydolph, 1977). The recent vegetation of eastern Georgia is part of the Irano–Turanian Group (Connor et al., 2004; Sagheb-Talebi et al., 2014). In the surroundings of Tbilisi, the natural vegetation is characterized by xerophytes and semidesert vegetation, while the vegetation on the southern slopes of the mid-mountain Kura-fold-and-thrust-belt changes from oak-hornbeam forest in the lower parts to mixed beech forests in the upper parts. In the semi-humid lowlands of the upper Alazani valley, the natural vegetation can be classified as elm-oak-vine forests. However, agricultural fields cover most of the valley today. The mid-mountain belt of the upper Alazani valley is characterized by mixed beech and hornbeam forests and in small parts also by fir-spruce forests (Connor and Kvavadze, 2008, Fig. 2B).

2.2 Leaf wax analyses

Analytical procedure

Leaf waxes were analysed at the Institute of Geography of the University of Bern/Switzerland. Free lipids from modern plant and topsoil samples were extracted using an ultrasonic treatment. Plant material (~1g) and soil material (~10g) were extracted three times with 20 ml dichloromethane (DCM): methanol (MeOH) (9:1, *v/v*) in an ultrasonic bath for 15 min.

The total lipid extract was separated over aminopropyl pipette columns into: i) the apolar fraction including the *n*-alkanes, ii) the polar fraction, and iii) the acid fraction. The *n*-alkanes were eluted with ~4 ml hexane and further purified over coupled silver-nitrate ($AgNO_3$-) - zeolite pipette columns. The *n*-alkanes trapped in the zeolite were subsequently dissolved in hydrofluoric acid and recovered by liquid-liquid extraction using *n*-hexane.

5   Afterwards, the *n*-alkanes were identified and quantified using a gas chromatograph with a flame ionisation detector (GC-FID). GC-FID measurements were performed on an Agilent 7890 gas-chromatograph equipped with an Agilent HP5MS column (30 m * 320 μm * 0.25 μm film thickness). For quantification and identification, external *n*-alkane standards (C_{21} – C_{40}) were run with each sequence.

Data analyses

10   *n*-Alkane concentrations were calculated as the sum of C_{25} and C_{35}, and given in μg g^{-1} dry weight.

Odd-over-even predominance (OEP) values (Eq. 1) were determined following Hoefs et al. (2002). Low values (<5) indicate an enhanced state of degradation (Buggle et al., 2010; Zech et al., 2009).

$$OEP = \frac{C27+C29+C31+C33}{C26+C28+C30+C32} \qquad (1)$$

The average chain length (ACL) of *n*-alkanes (Eq. 2) was calculated after Poynter et al. (1989), and was used to distinguish

15   between leaf waxes that predominantly originate from deciduous trees and shrubs (C_{27} and C_{29}; i.e. lower values) and those mainly originating from grass vegetation (C_{31} and C_{33}; i.e. higher values).

$$ACL = \frac{27*C27+29*C29+31*C31+33*C33}{C27+C29+C31+C33} \qquad (2)$$

The *n*-alkane ratio (Eq. 3) is a normalized ratio to differentiate between vegetation forms, with higher values for grasses and herbs and lower values for deciduous trees and shrubs.

20   $$n-\text{alkane ratio} = \frac{C31+C33}{C27+C29+C31+C33} \qquad (3)$$

3 Results

n-Alkanes are present in all analysed modern plant and topsoil samples from eastern Georgia, and the data are provided in the *supporting online material SOM-3*.

All samples show a distinct dominance of long odd-chained *n*-alkanes (>C_{25}). The total *n*-alkane concentrations (C_{25}-C_{35})

25   range from 1.1 to 299.1 μg g^{-1} sediment, and modern plant samples have higher *n*-alkane amounts than topsoil samples (Fig. 3a). All samples show distinct odd-over-even predominance (OEP) values between 3.1 and 18.7 (Fig. 3b). Samples from modern plant material show higher OEP values than topsoil material. Average-chain-length (ACL) values range from 28.6 to 31.2 (Fig. 3c). Differences in chain-length patterns are further reported by the *n*-alkane ratio that ranges from 0.16 to 0.77

(Fig. 3d). Lower *n*-alkane ratios (<0.5) are characteristic for the samples from deciduous sites, whereas higher ratios (>0.5) are typical for samples from grassland sites.

Furthermore, differences in the chain-lengths patterns between samples from deciduous sites and grassland sites are illustrated in Fig. 4. Samples from deciduous sites show a clear dominance of C_{29}, whereas samples from grassland sites are dominated by C_{31}. This pattern is characteristic for both, analysed modern plant and topsoil material, although the standard deviation of C_{29} and C_{31} is wider in the analysed modern plant samples (Fig. 4a).

4 Discussion

4.1 *n*-Alkane pattern in modern plants and topsoils

All modern plant and topsoil samples from eastern Georgia show a distinct/pronounced OEP that indicate their good preservation and prove their leaf wax origin (Eglinton and Hamilton, 1967). Higher *n*-alkane concentrations and OEPs are typical for fresh and non-degraded plant material, while the topsoils show lower concentrations and OEPs (Fig. 3a, b) that might indicate enhanced degradation (Buggle et al., 2010; Schäfer et al., 2016b). Although the degradation of organic matter (OM) already started in the topsoils, the OEP values in those samples are mostly not <5 which still indicates a good preservation of the *n*-alkanes and allows the reconstruction of former vegetation patterns. Accordingly, both the ACL and the *n*-alkane ratio report distinct differences in the chain-length patterns for sites with deciduous trees and grassland (Fig. 3, 4). Higher values and a C_{31} dominance are characteristic for *n*-alkanes from sites with grassland, whereas lower values and a dominance of C_{29} are characteristic for sites with deciduous trees (Fig. 3c, d).

However, modern plant samples 9p, 25p and 34p originating from sites with grassland show a chain-length dominance of C_{29}, whereas modern plant samples 3p and 29p and topsoil sample 23s originating from sites with deciduous trees are dominated by C_{31} homologues. Thus, these samples do not support the proposed chain-length patterns for the respective vegetation types. At the sampling site of topsoil sample 23s, hornbeam trees were only growing in patches and the site is and probably was intensively used for grazing activities. Thus, the dominance of C_{31} in the topsoil of this site is most likely an inherited signal from former land-use. Moreover, as turnover times of *n*-alkanes range in order of decades (Wiesenberg et al., 2004), land use and vegetation changes might actually be a possible explanation for the observed contradictory *n*-alkane pattern in the topsoil of this site. For modern plant samples it is possible that the described outliers reflect: (i) a large species-specific variability of the *n*-alkane pattern that was repeatedly reported in the literature (Bush and McInerney, 2013; Diefendorf et al., 2011) and/or (ii) an influence of annual temperatures (Tipple and Pagani, 2013; Bush and McInerney, 2015; Sachse et al., 2006) and hydroclimatic conditions (Hoffmann et al., 2013) on the homologue patterns. For example, modern plant samples from site 9 and 34 were taken in high altitudes of the Kura-fold-and-thrust-belt (1659 m a.s.l.) and in the floodplain of the upper Alazani Basin (445 m a.s.l.), respectively. These sites represent either extreme temperatures (site 9) or enhanced water availability (site 34) that might have affected the *n*-alkane synthesis at these locations. As the respective topsoil samples from sites 9 and 34 averaging the *n*-alkane patterns over several years/decades and show the expected C_{31}

dominance, modern plant samples probably record a more variable annual and/or monthly *n*-alkane pattern from these sites. This is also supported by the generally larger standard deviations of the *n*-alkane abundances from modern plant material taken at some of our studied sites.

Taken together, although it has recently been questioned whether *n*-alkane patterns originate from leaf waxes and are suitable to distinguish between different vegetation types at all (Bush and McInerney, 2013), our results from eastern Georgia confirm the leaf wax origin and chemotaxonomic discrimination power of the *n*-alkane pattern from modern plant and topsoil samples on a regional scale. Moreover, these results are in good agreement with previous transect studies from Central and South-Eastern Europe (Zech et al., 2009; Zech et al., 2013; Schäfer et al., 2016b). Thus, *n*-alkane patterns have a great potential to reconstruct paleovegetation when used in regional sedimentary archives.

4.2 Implications for reconstructing paleovegetation compositions

When using leaf wax *n*-alkanes in sedimentary archives, degradation of OM needs to be taken into account. Ongoing degradation leads to preferential losses of the most abundant homologues. Thus, changes of the homologue distribution and potentially confounding degradation effects can be visualized in an end-member model (Zech et al., 2009; Zech et al., 2013; Schäfer et al., 2016b) that is based on litter and topsoil samples from deciduous forests and grasslands in Europe. As illustrated in Fig. 5, our end-member model uses the normalized *n*-alkane ratio $(C_{31}+C_{33})/(C_{27}+C_{29}+C_{31}+C_{33})$ on the y-axis and the OEP on the x-axis. While the *n*-alkane ratio differentiates between vegetation with higher values for grasses and grassland soils and lower values for deciduous trees and deciduous forest soils, the OEP is used as a proxy for degradation. The respective trendlines, referred to as "degradation lines" for grass vegetation and deciduous trees, illustrate how the *n*-alkane ratio changes with degradation (Fig. 5). With increasing degradation, the degradation lines of grasses and deciduous trees converge and the discrimination power of the *n*-alkane ratio becomes less. The study of Schäfer et al. (2016b) uses a slightly different *n*-alkane ratio that excluded C_{29} and improved the discrimination power for their region. However, this is not the case for eastern Georgia were C_{29} and C_{31} are the most abundant homologues in our samples.

Our *n*-alkane samples from modern plants and topsoils from eastern Georgia show clear differences between sites with deciduous trees and those with grassland, and plot along the respective degradation lines of grasses and deciduous trees in the endmember plot (see Fig. 5). Thus, they are in good agreement with the reference samples from South-Eastern Europe that were presented in the end-member model of Zech et al. (2013). Accordingly, we integrated our *n*-alkane results from eastern Georgia into that dataset and recalculated the degradation lines. As mentioned above and illustrated in Fig. 5, some outliers of modern plants and topsoils from sites with deciduous trees plot in the direction of the grass degradation line and vice versa. These outliers can possibly be explained by mixed vegetation and anthropogenic land-use at the specific sites as well as temperature and hydroclimatic effects (see chapter 4.1). Thus, these samples are not exemplary and were not considered when adjusting the degradation lines.

The adjusted degradation lines can now be used to calculate the relative vegetation contributions of grasses and deciduous trees in paleosamples that were taken from sedimentary archives from the southern Caucasus and comparable regions. De-

pending on the vegetation type that contributed most to the sample, the *n*-alkanes will plot in the two-component mixing end-member model on or near to one of the degradation lines of grasses or deciduous trees, respectively. The percentage of grass can be calculated by the following formula:

$$\% \text{ grass} = \frac{n-\text{alkane ratio (sample)}-\text{equation (degradation line trees)}}{\text{equation (degradation lines grass)}-\text{equation (degradation lines trees)}} * 100 \qquad (4)$$

5 In principle, the accuracy of the correction is limited by the degradation state of a sample, i.e. it decreases with low OEPs and thus with converging degradation lines. Furthermore, numerical corrections can yield even negative or >100 %grass values, however the grass percentages should not be over-interpreted and instead be considered as semi-quantitative estimates. This effect is caused by the large scatter in the reference sample data set that can only be reduced towards more realistic values by integrating more regional reference samples into the end-member model as we did during our study.

10 Nevertheless, for more robust interpretations of *n*-alkane patterns (i.e. the ACL or ratios) in paleoapplications, they should be checked and corrected for degradation effects with regionally derived end-members.

5 Conclusions

This study systematically investigates long-chain *n*-alkanes in modern plant and topsoil material from eastern Georgia in the central southern Caucasus to test their potential for paleoenvironmental studies. Our results illustrate that:

15 i.) long-chain *n*-alkanes (C_{25}-C_{35}) originate from the leaf waxes of higher terrestrial plants and can thus serve as a valuable proxy that directly reflects the local vegetation.

ii.) The regional leaf wax *n*-alkane patterns show distinct and consistent differences between samples from sites with grassland and those with deciduous trees in eastern Georgia: Samples from grassland sites are characterized by a dominance of the homologue C_{31}, whereas samples from sites with deciduous trees show higher abundances of C_{29}.

20 Thus, leaf wax *n*-alkanes allow to differentiate between these two vegetation types and have a great potential for paleovegetation reconstructions in the semi-humid to semi-arid southern Caucasus region. However, the chain-length abundances might also be influenced by species-specific variability and environmental parameters, but these are only second-order effects at our investigated sites.

iii.) The degradation state of the *n*-alkanes has to be accounted for, given that increasing degradation reduces the

25 vegetation-specific differences in the *n*-alkane homologue patterns. Thus, we suggest an updated end-member model that corrects for these effects by including our plant and topsoil samples from eastern Georgia, and allows for a better correction of regional paleosamples.

Overall, our findings are in good agreement with other regional studies from Central and South-Eastern Europe and show the high potential of leaf wax *n*-alkanes for paleoenvironmental research applications. However, regional

30 calibration studies with modern reference samples are a necessary base for the robust interpretation of leaf wax derived long-chain *n*-alkanes in terms of former vegetation changes.

6 Data availability

The dataset that is used in this study is available via the supporting online material.

Acknowledgements

We thank Ulrich Göres (Dresden) and Giorgi Merebashvili (Tblisi) for their help during fieldwork. We thank Tobias Stalder
5 (Bern) for laboratory work. This project was financially supported by the Swiss National Science Foundation (PP00P2-150590).

References

Buggle, B., Wiesenberg, G. L., and Glaser, B.: Is there a possibility to correct fossil n-alkane data for postsedimentary altera-
10   tion effects?, Applied Geochemistry, 25, 947–957, doi:10.1016/j.apgeochem.2010.04.003, 2010.

Bush, R. T. and McInerney, F. A.: Leaf wax n-alkane distributions in and across modern plants: Implications for paleoecolo-
gy and chemotaxonomy, Geochimica et Cosmochimica Acta, 117, 161–179, doi:10.1016/j.gca.2013.04.016, 2013.

Bush, R. T. and McInerney, F. A.: Influence of temperature and C4 abundance on n-alkane chain length distributions across
the central USA, Organic Geochemistry, 79, 65–73, doi:10.1016/j.orggeochem.2014.12.003, 2015.

15 Connor, S. E. and Kvavadze, E. V.: Modelling late Quaternary changes in plant distribution, vegetation and climate using
pollen data from Georgia, Caucasus, Journal of Biogeography, 36, 529–545, doi:10.1111/j.1365-2699.2008.02019.x,
2008.

Connor, S. E., Thomas, I., Kvavadze, E. V., Arabuli, G. J., Avakov, G. S., and Sagona, A.: A survey of modern pollen and
vegetation along an altitudinal transect in southern Georgia, Caucasus region, Review of Palaeobotany and Palynology,
20   129, 229–250, doi:10.1016/j.revpalbo.2004.02.003, 2004.

Diefendorf, A. F., Freeman, K. H., Wing, S. L., and Graham, H. V.: Production of n-alkyl lipids in living plants and implica-
tions for the geologic past, Geochimica et Cosmochimica Acta, 75, 7472–7485, doi:10.1016/j.gca.2011.09.028, 2011.

Egeland, C. P., Gasparian, B., Fadem, C. M., Nahapetyan, S., Arakelyan, D., and Nicholson, C. M.: Bagratashen 1, a strati-
fied open-air Middle Paleolithic site in the Debed river valley of northeastern Armenia: A preliminary report, Archaeo-
25   logical Research in Asia, 8, 1–20, doi:10.1016/j.ara.2016.10.001, 2016.

Eglinton, G. and Hamilton, R. J.: Leaf Epicuticular Waxes, Science, 156, 1322–1335, doi:10.1126/science.156.3780.1322,
1967.

Eglinton, G., Hamilton, R. J., Raphael, R. A., and Gonzalez, A. G.: Hydrocarbon Constituents of the Wax Coatings of Plant
Leaves: A Taxonomic Survey, Nature, 193, 739–742, doi:10.1038/193739a0, 1962.

30 Eglinton, T. I. and Eglinton, G.: Molecular proxies for paleoclimatology, Earth and Planetary Science Letters, 275, 1–16,
doi:10.1016/j.epsl.2008.07.012, 2008.

Forte, A. M., Cowgill, E., Bernardin, T., Kreylos, O., and Hamann, B.: Late Cenozoic deformation of the Kura fold-thrust belt, southern Greater Caucasus, Geological Society of America Bulletin, 122, 465–486, doi:10.1130/B26464.1, 2010.

Hoefs, M. J., Rijpstra, W. C., and Sinninghe Damsté, J. S.: The influence of oxic degradation on the sedimentary biomarker record I: Evidence from Madeira Abyssal Plain turbidites, Geochimica et Cosmochimica Acta, 66, 2719–2735, doi:10.1016/S0016-7037(02)00864-5, 2002.

Hoffmann, B., Kahmen, A., Cernusak, L. A., Arndt, S. K., and Sachse, D.: Abundance and distribution of leaf wax n-alkanes in leaves of Acacia and Eucalyptus trees along a strong humidity gradient in northern Australia, Organic Geochemistry, 62, 62–67, doi:10.1016/j.orggeochem.2013.07.003, 2013.

Joannin, S., Ali, A., Ollivier, V., Roiron, P., Peyron, O., Chevaux, S., Nahapetyan, S., Tozalakyan, P., Karakhanyan, A., and Chataigner, C.: Vegetation, fire and climate history of the Lesser Caucasus: A new Holocene record from Zarishat fen (Armenia), J. Quaternary Sci., 29, 70–82, doi:10.1002/jqs.2679, 2014.

Kolattukudy, P. E. and Walton, T. J.: The biochemistry of plant cuticular lipids, Progress in the Chemistry of Fats and other Lipids, 13, 119–175, doi:10.1016/0079-6832(73)90006-2, 1973.

Liu, W. and Huang, Y.: Compound specific D/H ratios and molecular distributions of higher plant leaf waxes as novel paleoenvironmental indicators in the Chinese Loess Plateau, Organic Geochemistry, 36, 851–860, doi:10.1016/j.orggeochem.2005.01.006, 2005.

Lydolph, P. E. (Ed.): Climates of the Soviet Union: [138 Tab.], World survey of climatology, 7, Elsevier, Amsterdam, 443 pp., 1977.

Marseille, F., Disnar, J. R., Guillet, B., and Noack, Y.: n-Alkanes and free fatty acids in humus and A1 horizons of soils under beech, spruce and grass in the Massif-Central (Mont-Lozère), France, European Journal of Soil Science, 50, 433–441, doi:10.1046/j.1365-2389.1999.00243.x, 1999.

Messager, E., Belmecheri, S., Grafenstein, U. von, Nomade, S., Ollivier, V., Voinchet, P., Puaud, S., Courtin-Nomade, A., Guillou, H., Mgeladze, A., Dumoulin, J.-P., Mazuy, A., and Lordkipanidze, D.: Late Quaternary record of the vegetation and catchment-related changes from Lake Paravani (Javakheti, South Caucasus), Quaternary Science Reviews, 77, 125–140, doi:10.1016/j.quascirev.2013.07.011, 2013.

Poynter, J. G., Farrimond, P., Robinson, N., and Eglinton, G.: Aeolian-Derived Higher Plant Lipids in the Marine Sedimentary Record: Links with Palaeoclimate, in: Paleoclimatology and Paleometeorology: Modern and Past Patterns of Global Atmospheric Transport, Leinen, M., and Sarnthein, M. (Eds.), Springer Netherlands, Dordrecht, 435–462, 1989.

Sachse, D., Radke, J., and Gleixner, G.: δD values of individual n-alkanes from terrestrial plants along a climatic gradient – Implications for the sedimentary biomarker record, Organic Geochemistry, 37, 469–483, doi:10.1016/j.orggeochem.2005.12.003, 2006.

Sagheb-Talebi, K., Sajedi, T., and Pourhashemi, M.: Forests of Iran: A treasure from the past, a hope for the future, Plant and Vegetation, 10, Springer Netherlands, Dordrecht, s.l., 55 pp., 2014.

Schäfer, I. K., Bliedtner, M., Wolf, D., Faust, D., and Zech, R.: Evidence for humid conditions during the last glacial from leaf wax patterns in the loess–paleosol sequence El Paraíso, Central Spain, Quaternary International, doi:10.1016/j.quaint.2016.01.061, 2016a.

Schäfer, I. K., Lanny, V., Franke, J., Eglinton, T. I., Zech, M., Vysloužilová, B., and Zech, R.: Leaf waxes in litter and top-soils along a European transect, SOIL, 2, 551–564, doi:10.5194/soil-2-551-2016, 2016b.

Schatz, A.-K., Zech, M., Buggle, B., Gulyás, S., Hambach, U., Marković, S. B., Sümegi, P., and Scholten, T.: The late Quaternary loess record of Tokaj, Hungary: Reconstructing palaeoenvironment, vegetation and climate using stable C and N isotopes and biomarkers, Quaternary International, 240, 52–61, doi:10.1016/j.quaint.2010.10.009, 2011.

Schefuß, E., Schouten, S., Jansen, J. H. F., and Sinninghe Damsté, J. S.: African vegetation controlled by tropical sea surface temperatures in the mid-Pleistocene period, Nature, 422, 418–421, doi:10.1038/nature01500, 2003.

Schwark, L., Zink, K., and Lechterbeck, J.: Reconstruction of postglacial to early Holocene vegetation history in terrestrial Central Europe via cuticular lipid biomarkers and pollen records from lake sediments, Geol, 30, 463, doi:10.1130/0091-7613(2002)030<0463:ROPTEH>2.0.CO;2, 2002.

Suchodoletz, H. von, Menz, M., Kühn, P., Sukhishvili, L., and Faust, D.: Fluvial sediments of the Algeti River in southeast-ern Georgia — An archive of Late Quaternary landscape activity and stability in the Transcaucasian region, Catena, 130, 95–107, doi:10.1016/j.catena.2014.06.019, 2015.

Tipple, B. J. and Pagani, M.: Environmental control on eastern broadleaf forest species' leaf wax distributions and D/H rati-os, Geochimica et Cosmochimica Acta, 111, 64–77, doi:10.1016/j.gca.2012.10.042, 2013.

Wiesenberg, G. L., Schwarzbauer, J., Schmidt, M. W., and Schwark, L.: Source and turnover of organic matter in agricultur-al soils derived from n-alkane/n-carboxylic acid compositions and C-isotope signatures, Organic Geochemistry, 35, 1371–1393, doi:10.1016/j.orggeochem.2004.03.009, 2004.

Wolf, D., Baumgart, P., Meszner, S., Fülling, A., Haubold, F., Sahakyan, L., Meliksetian, K., and Faust, D.: Loess in Arme-nia – stratigraphic findings and palaeoenvironmental indications, Proceedings of the Geologists' Association, 127, 29–39, doi:10.1016/j.pgeola.2016.02.002, 2016.

Zech, M., Buggle, B., Leiber, K., Marković, S., Glaser, B., Hambach, U., Huwe, B., Stevens, T., Sümegi, P., Wiesenberg, G., and Zöller, L.: Reconstructing Quaternary vegetation history in the Carpathian Basin, SE-Europe, using n-alkane bi-omarkers as molecular fossils, E&G – Quaternary Science Journal; Vol. 58 No 2; 148-155; ISSN 0424-7116, doi:10.3285/eg.58.2.03, 2009.

Zech, R., Zech, M., Marković, S., Hambach, U., and Huang, Y.: Humid glacials, arid interglacials?: Critical thoughts on pedogenesis and paleoclimate based on multi-proxy analyses of the loess–paleosol sequence Crvenka, Northern Serbia, Palaeogeography, Palaeoclimatology, Palaeoecology, 387, 165–175, doi:10.1016/j.palaeo.2013.07.023, 2013.

Zhang, Z., Zhao, M., Eglinton, G., Lu, H., and Huang, C.: Leaf wax lipids as paleovegetational and paleoenvironmental proxies for the Chinese Loess Plateau over the last 170kyr, Quaternary Science Reviews, 25, 575–594, doi:10.1016/j.quascirev.2005.03.009, 2006.

5   **Figure 1: Overview of the Caucasus Region. The red rectangle marks the study area.**
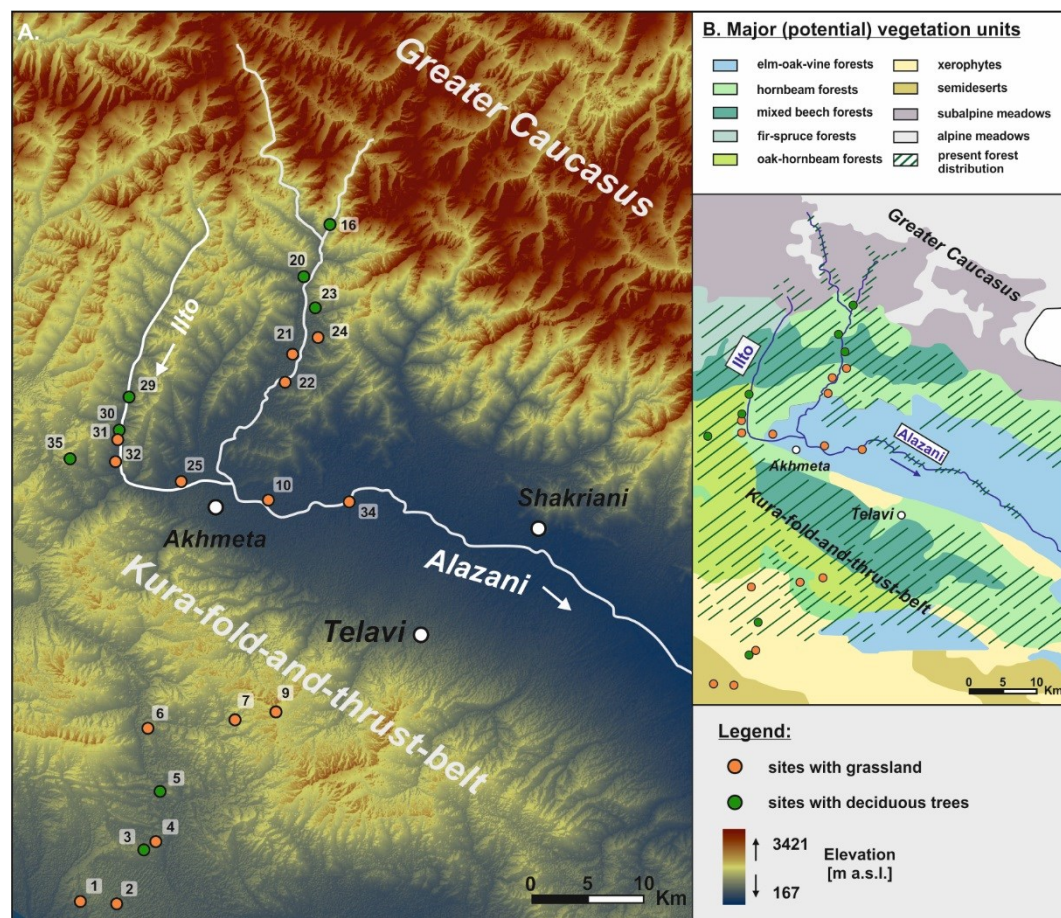
Figure 2: A. Digital elevation model of the study area (Aster DEM). Locations of plant and topsoil samples are indicated by an orange dot for sites with grassland, and a green dot for sites with deciduous trees. B. Current natural vegetation in the study area (based on the bioclimatic map of Connor & Kvavadze 2008). The current distribution of forests in the study area (second half of 20th century) is derived from Soviet military maps 1:200,000.
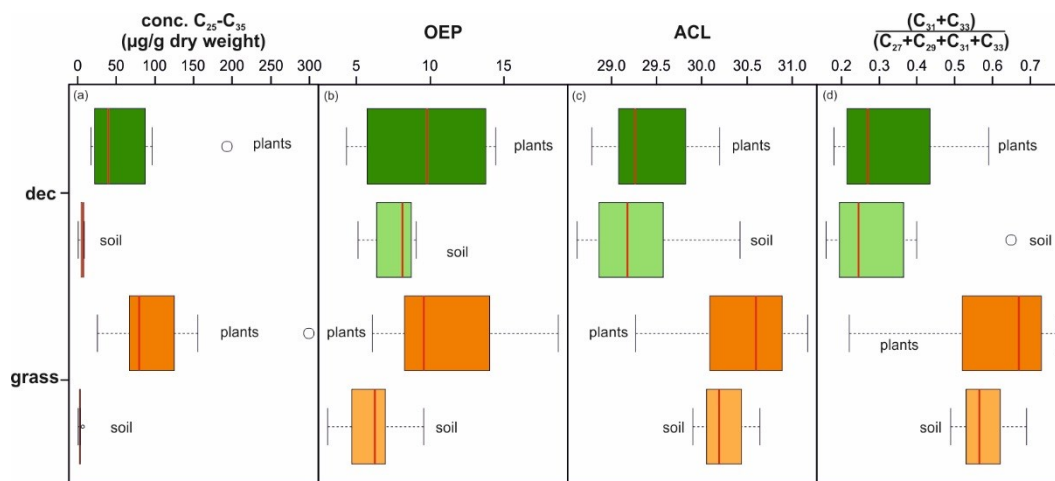
Figure 3: Box plots of *n*-alkanes from modern plant and topsoil samples. (a) Concentration ug/g (C₂₅-C₃₅), (b) Odd-over-even pre-dominance (OEP), (c) Average chain length (ACL), (d) *n*-alkane ratio (C₃₁+C₃₃)/(C₂₇+C₂₉+C₃₁+C₃₃). Dec = deciduous sites (n = 16); grass = grassland sites (n = 28). Box plots show median (red line), interquartile range (IQR) with upper (75 %) and lower (25 %) quartiles.
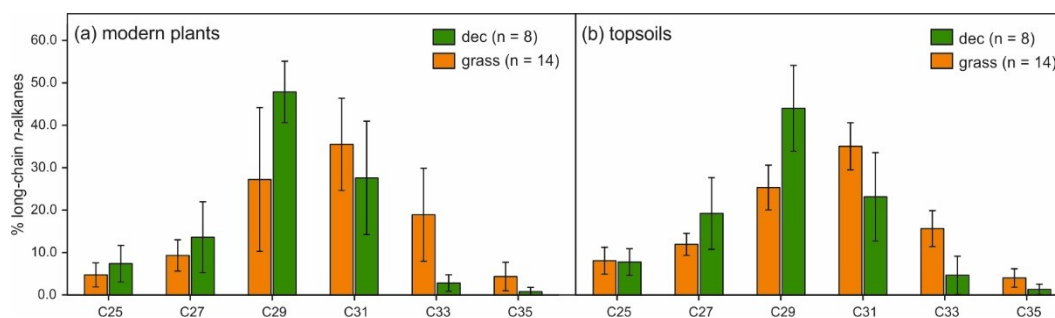
Figure 4: Chain length distribution patterns for long-chain *n*-alkanes from sites with deciduous trees and with grassland in (a) modern plants and (b) topsoils.
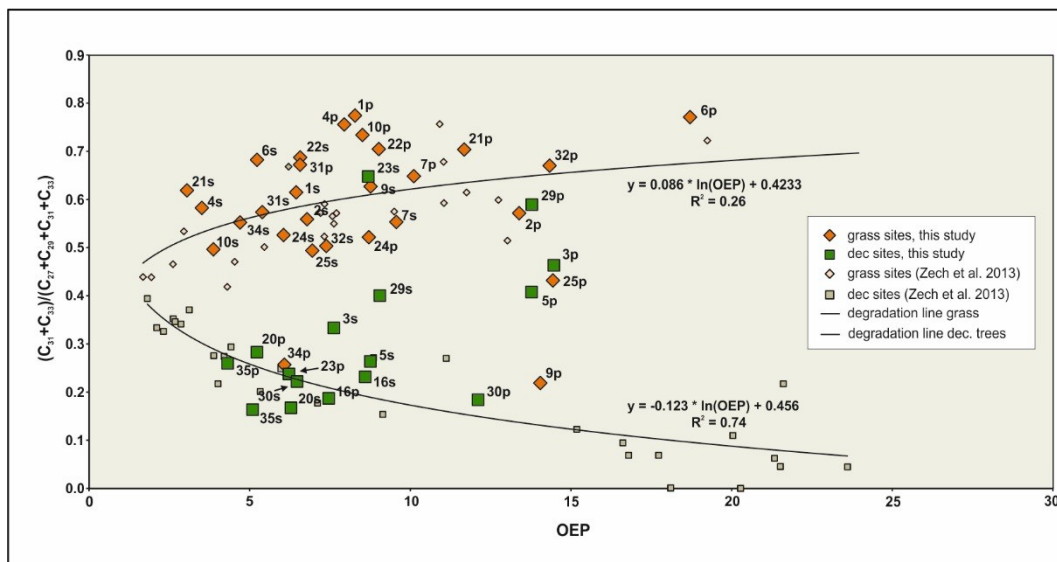
Figure 5: End-member plot for the *n*-alkane ratio (C₃₁+C₃₃)/(C₂₇+C₂₉+C₃₁+C₃₃). *n*-Alkane results from plant and topsoil samples from the upper Alazani catchment were integrated into a dataset from recent grassland and forest sites from Europe (R. Zech et al., 2013). Degradation line for grass: y = 0.086 * ln(OEP) + 0.4233. Degradation line for tress, with y = -0.123 * ln(OEP) + 0.456.